2015 8th International Congress on Image and Signal Processing (CISP 2015)

Lighting Difference based Wrinkle Mapping for Expression Synthesis

Weicheng Xie*, Linlin Shen*, Meng Yang*, Qibin Hou†
*School of Computer Science & Software Engineering, Shenzhen University, China
{wcxie, llshen}@szu.edu.cn
†Ningbo Augvision Digital Tech Ltd., China
qbhou@augvision.com.cn

***Abstract*—Nowadays, facial expression synthesis is widely used in expression simulation, recognition and animation. Texture feature (wrinkle) after face deformation largely reflects the genuineness of the synthesized expression, whose mapping is a critical step to the expression synthesis application. However, current lighting ratio based wrinkle mapping is sensitive to small source lighting and large lighting difference. In this work, a novel wrinkle mapping based on lighting difference fitting is proposed to improve the genuineness and robustness of mapped wrinkles. Experimental results on expression synthesis with large lighting difference show that the proposed algorithm is competitive on synthesizing visually genuine expressions.**

I. Introduction

With the development of face recognition and facial animation, expression synthesis has been increasingly important and widely used in these applications. Low-quality 2D images and 3D depth maps were mapped to realistic facial expressions by optimization with geometry and texture registration [1]. Features of 2D geometric deformation were employed for the facial expression recognition [2], where 2D deformable models tracking the greatest facial expression intensity were used for SVM classification. Other algorithms related with facial deformation and synthesis for expression recognition were also reported in [3], [4], [5]. Generally, the algorithms of expression synthesis are mainly divided into two categories, the 3D based and the 2D based.

The 3D based expression synthesis often requires a matching between 2D image and 3D shape or a database of basic expression set with respect to (w.r.t.) the target person, which is time consuming.

Unlike the 3D based expression synthesis, the 2D based algorithms learn geometry and texture features of the reference (source) expressions and map these features directly onto the target face. According to the type of the reference expressions, the 2D based algorithms are classified into two classes, one class is based on statistical learning of multiple reference expressions, the other is based on face deformation and wrinkle mapping which demands a single expression.

The statistically based algorithms generally require the following steps:

- Extract the corresponding feature points on faces of source neutral (F_{sn}), source expression (F_{se}) and target neutral (F_{tn});
- Divide the face region into small parts and extract the regions containing expression features;
- Based on a source expression for simulating or a database of expressions w.r.t. the considered person, synthesize or simulate the new expression.

In the work of Beymer et al. [6], the synthesis of the expression was divided into phases of analysis and synthesis. The principle component analysis (PCA) was used to simulate new expressions by changing the coefficients of principle components corresponding to the expression feature points [7]. This method adopted facial region segmentation and interpolation to simulate the wrinkles on the face. However, it may not work when the size of the face is largely changed. Methods of bilinear kernel regression [8] and facial animation parameters (FAPs) [9] were also employed for the statistically modeling of the expression synthesis. For statistically based algorithms, a database of referred expressions w.r.t. the considered person is needed in general, and these methods mainly concentrate on the detail preservation of the generated expression.

The deformation and mapping based algorithms generally require the following steps:

- Location and alignment of the feature points on faces of F_{sn}, F_{se} and F_{tn};
- Deformation of the target face F_{tn} by learning the movement from F_{sn} and F_{se};
- Wrinkle mapping on the deformed face of F_{tn}.

A. Correspondence Matching and Face Deformation

For the aspect of face correspondence, Liu et al. [10] and Zhang et al. [11] located the positions and correspondence of the feature points manually. Song et al. [12] made this step semi-automatic. Actually, this step can be made more automatic by employing face alignment algorithms, such as the optical flow employed by Li et al. [13], the minimization optimization of an energy function proposed by Qian et al. [14] and Liao et al. [15] and cascade of regression trees adopted in [16], [17].

For 2D deformation algorithms, there were some interpolation based deformation [7], [8], while the obtained deformation shape is apt to lose some geometry features on the non-feature points. The wrapping algorithm in [18] obtained the weighted movement of each pixel, which was adopted in the expression synthesis algorithms [10], [12] for the face mesh

978-1-4673-9098-9/15/$31.00 ©2015 IEEE

deformation. The feature points on the deformed target face were approximated with the weighted positions of the feature points by an elastic model [11]. A global optimization model for 2D shape deformation was presented in [19].

B. Wrinkle Mapping

For the aspect of wrinkle mapping, unlike the 3D wrinkle generation [20], [21] by modeling wrinkles and deformation for the 3D expression synthesis, the 2D wrinkle simulation needs only learn and map the reference wrinkle features. Liu et al. [10] constructed a method for preserving the facial characteristics (e.g. the wrinkles), where the expression ratio image (ERI) between F_{sn} and F_{se} was assumed to be the same as that between F_{tn} and F_{te}. The expression features with ERI was mapped to the retrieved and deformed face sequence to obtain the final expression sequence [13]. Shift ERI incorporated with Gaussian damping weighting term was employed to map the wrinkles onto the target face [11]. These ratio based algorithms of lighting mapping are largely influenced by the abnormal lighting ratios when the lighting values of pixels on F_{sn} is relatively small. To avoid this disadvantage, we adopt the difference of the lightings [22] rather than the ratio between corresponding pixels on F_{sn} and F_{se} to simulate the lighting changes on the synthesized object. Moreover, a fitting form of the lighting difference is proposed.

In this work, a novel wrinkle mapping incorporating with mesh deformation (abbreviated as DaWF) is proposed to synthesize the facial expressions. The main contribution of the proposed DaWF concentrates on the ability of generating more genuine expressions in the stage of wrinkle mapping by solving a system of linear equations to fit lighting differences. Comparative results with several related algorithms in Section III-A reveal that the proposed mapping method can generate more complete wrinkle and is both robust and efficient.

This paper is structured as follows. Section II gives a description about the proposed algorithm step by step. The experimental results of the proposed algorithm on varieties of expressions are presented in Section III. Finally, discussions and some conclusions are addressed in Section IV.

II. The Proposed Algorithm

A. Framework of the Algorithm

As presented in Fig. 1, the general framework of the proposed DaWF consists of three steps. In the first step, the correspondence feature points are located and slightly adjustment. In the second step, we obtain the deformed geometry by mesh deformation. The wrinkles are mapped onto the deformed face in the last step.

B. Feature Location

As shown in Fig. 1(b), we view the whole face as a structure $\Gamma = \{\Gamma_1, \cdots, \Gamma_n\}$ which consists of eight parts i.e. two eyes, two brows, nose, mouse, lip and profile. For the feature location, active shape model (ASM) [23] is first employed to obtain the initial positions of these feature points including forehead region. Fig. 1(b) shows the location of the 79 feature

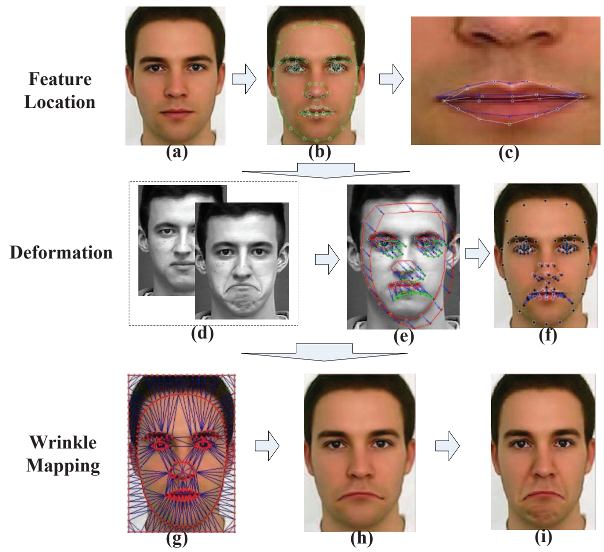

Fig. 1: The framework of the proposed algorithm.

points. However, the location is not accurate enough for the expression synthesis with large deformation. Thus, face part based active appearance model (AAM) [24] is employed to locate more accurate 68 feature points along part boundary edges, which are further used to trim the initial feature points on part boundary.

C. Mesh Deformation

The procedure of generating the feature points on F_{te} is divided into three steps.

In the first step, point alignment is performed to avoid the influence of rotation. All the feature points are first rotated to an unified coordinate system with reference to the positions of the two eyes and the nose on the F_{sn} and F_{tn} faces.

In the second step, initial positions of feature points on F_{te} are obtained according to the movements of feature points on F_{sn} and F_{se}, as demonstrated in Fig. 1(d),(e).

Given the central point of each part ($CP^{sn}_{(i)}$, $CP^{tn}_{(i)}$), the widths ($W^{(i)}_{sn}$, $W^{(i)}_{tn}$) and the heights ($H^{(i)}_{sn}$, $H^{(i)}_{tn}$) in the unified coordinate framework of the faces F_{sn}, F_{tn}, the positions of the feature points on F_{te} are estimated as follows:

$$V^{te}_{(i,j)} = CP^{tn}_{(i)} + (V^{se}_{(i,j)} - CP^{sn}_{(i)}) \begin{pmatrix} \frac{W^{(i)}_{tn}}{W^{(i)}_{sn}} & \\ & \frac{H^{(i)}_{tn}}{H^{(i)}_{sn}} \end{pmatrix}. \quad (1)$$

where $V^{te}_{(i,j)}$ denotes the j-th feature points on the i-th part on the face F_{te}.

Finally, the algorithm of mesh deformation [11] with elastic model is employed to obtain the final deformation triangular mesh using the target feature points $V^{te}_{(i,j)}$. The initial triangular mesh of F_{tn} and the corresponding deformation face are presented in Figs. 1(g),(h), respectively, where the deformed face is further used for wrinkle mapping the following section.

D. Wrinkle Mapping Based on Lighting Difference Fitting

After the deformation of the parts, the texture details (such as the wrinkle) are needed to be mapped onto the target expression face. In the work [10], the wrinkle was reflected as the lighting variants at the pixel (the Y component of the YUV colors). They further proposed a pixel-by-pixel assignment form to simulate the lighting of the pixel on the face F_{te} in equation (2):

$$\mathcal{B}'(u,v) = \mathcal{B}(u,v)ERI_{u,v}, \text{with } ERI_{u,v} = \frac{\mathcal{A}'(u,v)}{\mathcal{A}(u,v)}. \quad (2)$$

where $\mathcal{A}(u,v)$, $\mathcal{A}'(u,v)$ and $\mathcal{B}(u,v)$ correspond to the lighting intensities of F_{sn},F_{se} and F_{tn}, respectively.

The formula in equation (2) is based on the ratio of the lightings, and each pixel on F_{te} learns the lighting change from only one corresponding pixel on F_{se}. In the following, a difference based lighting mapping is introduced and implemented by solving a system of linear equations, where each pixel learns from the lighting differences of the adjacent eight pixels and this method is robust from abnormal lighting ratios when the pixel lighting $\mathcal{A}(u,v)$ is relatively small.

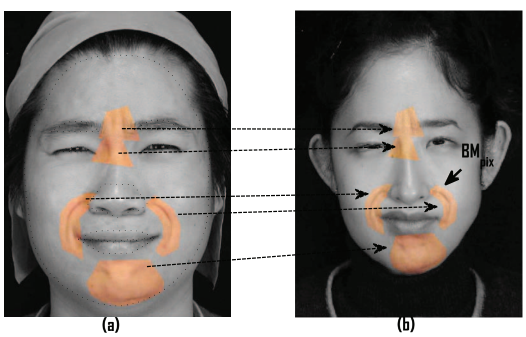

Fig. 2: The extraction and correspondence of wrinkle regions. (a): The extraction of wrinkle regions on F_{se} with colorized label. (b): The corresponding wrinkle regions BM_{pix} on F_{te}.

First, the regions on the face F_{te} where the wrinkles need to be manually extracted and mapped, which are denoted as BM_{pix}. Fig. 2 demonstrates the extraction and mapping of wrinkle regions. The corresponding lightings of faces F_{sn},F_{se},F_{tn} in the 3×3 adjacent region around the position (p,q) are denoted as $\{l^{(sn)}_{p,q}, l^{(se)}_{p,q}, l^{(tn)}_{p,q}; i-1 \le p \le i+1, j-1 \le q \le j+1\}$. Then the corresponding lightings on the face F_{te} are assumed to satisfy the constraints in equation (3)-(4).

For $(i,j) \in BM_{pix}$

$$\left\{ \begin{array}{l} (l^{(te)}_{p,q} - l^{(te)}_{i,j}) = (l^{(tn)}_{p,q} - l^{(tn)}_{i,j}) + \\ \qquad\qquad \lambda_r \cdot [(l^{(se)}_{p,q} - l^{(se)}_{i,j}) - (l^{(sn)}_{p,q} - l^{(sn)}_{i,j})], \\ i-1 \le p \le i+1, j-1 \le q \le j+1. \end{array} \right. \quad (3)$$

where $\lambda_r = \frac{CE_{t,r}}{CE_{s,r}}$, $CE_{s,r}, CE_{t,r}$ are the changed extents of lightings of the r-th wrinkle region on F_{sn},F_{tn}, respectively, which are approximated by the difference of the 95% largest and 5% largest lightings of each region BM_{pix} to alleviate the influence of the abnormal lightings.

For $(i,j) \notin BM_{pix}$

$$l^{(te)}_{i,j} = l^{(tn)}_{i,j}. \quad (4)$$

The equation (3) incorporating with equation (4) are then converted into one whole system of linear equations:

$$\left\{ \begin{array}{l} A \cdot L|_{BM_{pix}} = B \\ L|_{\overline{BM_{pix}}} = L_0 \end{array} \right. \quad (5)$$

where $L = \{l^{(te)}_{i,j}, (i,j) \in BM_{pix}\}$, A, B correspond to the coefficient matrixes constructed by equation (3), $\overline{BM_{pix}} = \Omega - BM_{pix}$ and Ω is entire facial region, L_0 records the corresponding lightings on the face F_{tn}. The least squares of this system $(A^T \cdot A) \cdot L = A^T \cdot B$ is then solved by the sparse LU decomposition.

Equation (5) is not well formulated when the lighting differences between F_{se} and F_{sn} along edges of wrinkle regions are significant, which makes the mapped wrinkles look not genuine enough on these edges. Thus, attenuation weight coefficient $\lambda_r(d)$ is introduced to substitute for λ_r in equation (3), which is defined as follows:

$$\lambda_r(d) = \left\{ \begin{array}{ll} \lambda_r \cdot sin(\frac{\pi}{2} \cdot \frac{d}{d_0}), & d \le d_0 \\ \lambda_r, & d > d_0 \end{array} \right. \quad (6)$$

where d is the distance between the considered pixel in the wrinkle region and the nearest edge, $d_0 = 5$ is a critical distance, λ_r is the r-th lighting ratio which is defined in equation (3).

III. Experimental Results

We perform the experiments on a PC with a 3.2GHZ core processor and 4 GB RAM. The set of all the expressions used in this test is shown in Fig. 3, where (a) shows an average man face downloaded from web, (b),(c) and the last row of expressions are neutral face images and the corresponding smile, sad and chuckle expression images used in paper [10] for testing. The expression of (d),(e) are faces of the 116-th person in the database [25].

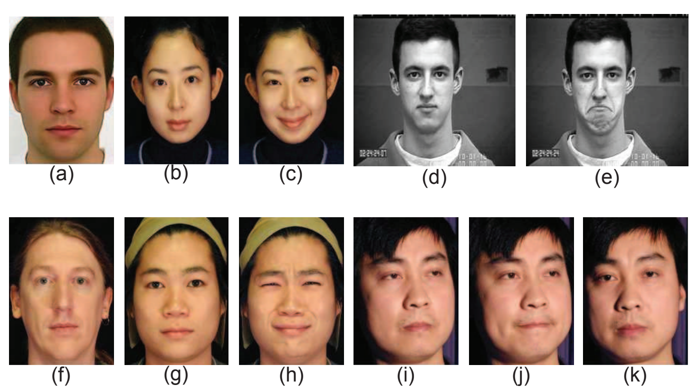

Fig. 3: The expression set used in the experimental test.

(a) (b)

Fig. 4: (a),(b): The neutral and synthesized $sad1$ expression of a little girl using Fig. 3(g) and (h) as F_{sn} and F_{se}.

(a) (b)

Fig. 5: (a),(b): The neutral and synthesized smile expression of a middle-aged man using Fig. 3(b) and (c) as F_{sn} and F_{se}.

(a) (b)

Fig. 6: (a),(b): The neutral and synthesized $sad2$ expression of the average man using Fig. 3(d) and (e) as F_{sn} and F_{se}.

A. Results of Wrinkle Mapping

To test the wrinkle mapping performance in overall, Figs. 4-6 present the results of sad ($sad1$), smile and sad ($sad2$) expressions mapped onto a little girl, a middle-aged man and an average man, when Figs. 3(g),(b),(d) are used as F_{sn} and Figs. 3(h),(c),(e) are used as F_{se}. The $sad1$ expression in Fig. 3(h) implies the deformations of the face profile, eyes and the mouth, which generate wrinkles on the regions between two brows and eyes, the cheeks and the lower jaw. It can be seen from Fig. 4(a),(b) that the geometry shape and the wrinkles are synthesized properly. The wrinkles on left mouth tip of the smiling face of Fig. 3(c) are not obvious, the proposed DaWF preserves this detail in Fig. 5(b). The wrinkle texture on two face cheeks and chin region of $sad2$ expression in Fig. 3(e) are complicated and chaotic, the proposed mapping form preserves these features genuinely in Fig. 6(b).

B. Comparison with Related Algorithms

Three related algorithms, i.e. expression ration image (ERI) [10], vertex tent coordinate [12] and musical model (MD) [11] are chosen here for comparison.

1) Metrics for Comparison: To compare the performance quantitatively, a metric formulated in equation (7) is defined as the correlation of the lighting differences between the source and synthesized faces, which reflects the similarity of F_{se} and F_{te}.

$$CorD = \frac{< \nabla L_{src}, \nabla L_{syn} >}{||\nabla L_{src}||_2 \cdot ||\nabla L_{syn}||_2}. \tag{7}$$

where $< \cdot, \cdot >$ is the inner product of two vectors.

The overall runtime (RT) of expression synthesis is also considered in the comparison, where the time cost on extracting the wrinkle regions is not included, as all the considered algorithms need to manually determine the locations of wrinkle regions. For the programming implementation, hybrid of MATLAB and C++ is employed to make use of the advantage of MATLAB software at the matrix computation and the efficiency of C++ at loop iteration. The smoothing operator and lighting mapping in ERI, the lighting mapping with shift ERI in MD algorithm and the procedures of constructing coefficient matrices in VTC and DaWF are coded in C++ to accelerate the implementation.

2) Visual Inspection: Fig. 7 presents the comparative results of our algorithm with several related algorithms on $sad1$ expression synthesis using Fig. 3(g),(h) and (b) as F_{sn}, F_{se} and F_{tn}, respectively. In this experimental test, the mesh deformation in the algorithm MD [11] was used for all competing approaches.

From the aspect of visual performance, it is demonstrated in Figs. 7(a)-(e) that the proposed DaWF preserves more complete wrinkles than the other algorithms on the cheek region. To demonstrate the detailed information of these algorithms on lighting preservation, Fig. 7(f)-(j) present lighting differences between the source and synthesized expressions on the region between two eyes, two cheeks and the lower jaw by different algorithms. One can observe from Figs. 7(g)-(j)

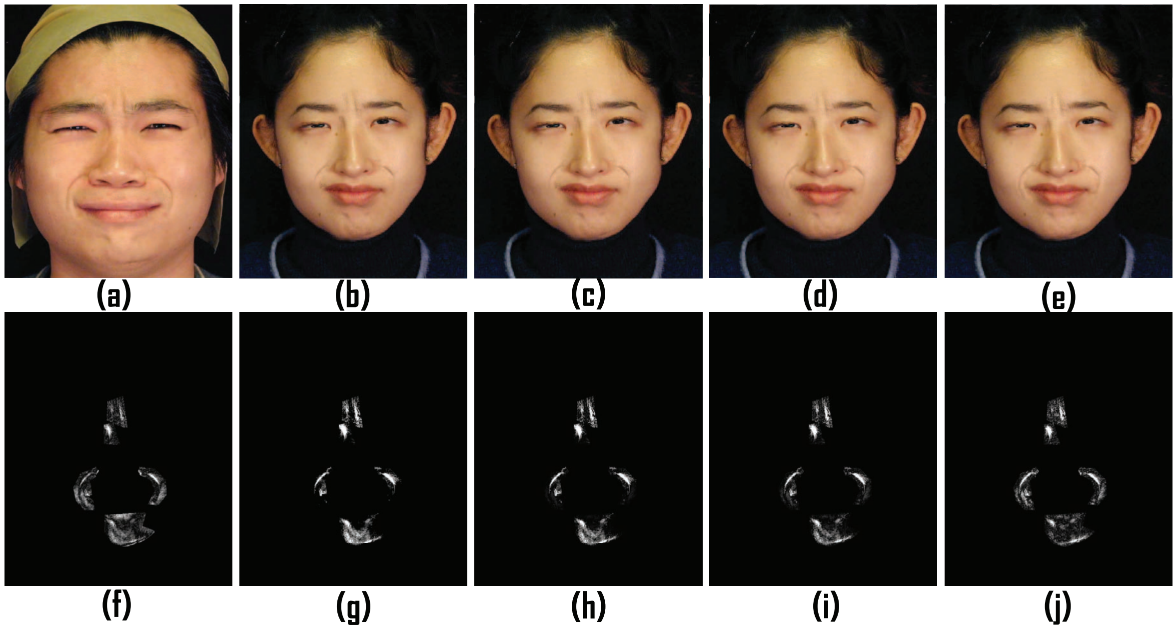

Fig. 7: The comparison of four algorithms on wrinkle mapping. (a) is the source sad expression, (b)-(e) are synthesized sad expressions obtained by the algorithm ERI [10], VTC [12], MD [11] and the proposed DaWF, respectively. (f) reflects the lighting difference between F_{sn} and F_{se} on four key wrinkle regions, (g)-(j) demonstrate the lighting differences between F_{tn} and F_{te} by the algorithms ERI, VTC, MD, DaWF, respectively.

TABLE I: Comparative results of the proposed algorithm and other algorithms in literature.

Algorithm	$RT(s)$ ($sad1$, Smile, $sad2$)	$CorD$ ($sad1$, Smile, $sad2$)	Preprocessing Needed	Lighting Mapping	Additional Parameters
ERI [10]	(8.4, 2.4, 1.0)	(0.74, 0.76, 0.69)	Smoothness filtering	ERI	c
VTC [12]	(12.3, 2.1, **0.8**)	(0.83, **0.82**, 0.73)	Correspondence modification	Covariance of ratios	-
MD [11]	(**7.9**, 2.5, 0.9)	(0.81, 0.82, 0.72)	A database of expressions	Shift ERI	$h(u_0, v_0)$, λ_k, w_{db}, $r(u_0, v_0)$
DaWF	(9.6, **2.0**, 0.8)	(**0.87**, 0.79, **0.75**)	Correspondence modification	Lighting difference	λ_1-λ_3

that the wrinkle difference obtained by the proposed DaWF is more similar to that of Fig. 7(f) than the other algorithms.

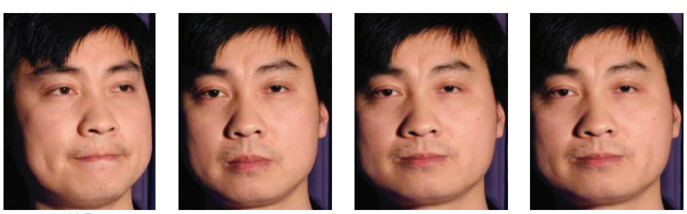

(a) F_{se} (b) F_{tn} (c) ERI Mapping (d) The Proposed

Fig. 8: The comparison of ERI and the proposed mappings for a non-frontal expression synthesis.

In the paper [10], Figs. 3(i),(j),(k) with non-obvious dimple wrinkles were used to test the algorithm performance on synthesizing frontal expression learning from non-frontal wrinkle features, where ERI format was reported to lose efficiency. In this work, we use Figs. 3(i),(j),(k) as F_{sn}, F_{se} and F_{tn} for the testing. It can be seen from Fig. 8(d) that the proposed wrinkle mapping still achieves distinct wrinkle features on the left cheek, which further illustrates that the proposed mapping outperforms ERI mapping on preserving non-obvious expression features.

Tab. I lists the comparative results of these algorithms in terms of RT and $CorD$ on $sad1$, smile, and $sad2$ expression synthesis using Figs. 3(g),(b),(d) as F_{sn}, Figs. 3(h),(c),(e) as F_{se}, and Figs. 3(b),(f),(a) as F_{tn}. The image sizes for the expressions of $sad1$, smile and $sad2$ are 746×621, 633×469 and 207×146, respectively.

Considering the overall runtime of expression synthesis, fitting-based algorithms VTC and DaWF outperform ERI based algorithms when the image size is small because the overall smoothness operation is not needed, which can be seen from RT values of smile expression synthesis in Tab. I.

Considering the metric of similarity, the difference form of the lighting adopted in the proposed DaWF achieves comparable results with the other algorithms. The proposed DaWF attempts to preserve the difference of lightings which is insensitive to abnormal lighting ratios, it is more robust and can map subtle lighting differences when the lighting $l_{i,j}^{sn}$ on F_{sn} is small. One can observe from $CorD$ values in Tab. I that DaWF achieves relatively better performance than the other algorithms.

IV. Discussion and Conclusion

In this work, an algorithm of expression synthesis (DaWF) with a novel strategy of wrinkle mapping is proposed, which is based on the fitting of lighting differences. Experimental results on various kinds of expressions and comparison with state-of-the-art algorithms illustrate the effectiveness and robustness of the wrinkle mapping method on detail preservation.

Although visually genuine expressions are synthesized by the proposed algorithm, there are still much margin for further improvements. Firstly, expression wrinkles need be detected automatically or semi-automatically to make it ease to use. Secondly, the algorithm of view morphing in [26] or 3D reconstruction algorithm in [27] can be integrated to synthesize expressions for largely rotated face in 3D space. Lastly, more efficient algorithm of mesh deformation should be devised to apply the proposed algorithm on expressions with large geometry deformation.

Acknowledgment

The work was supported by Natural Science Foundation of China under grand no. 61272050 and 61402289, China Postdoctoral Science Foundation under grant no. 2015M572363, the Science Foundation of Guangdong Province under grant no. 2014A030313556 and 2014A030313558, Shenzhen Scientific Research and Development Funding Program (Grant no. JCYJ20140509172609171), Scientific Research Fund for new teacher of Shenzhen University (Grant no. 201536), Scientific Research fund for Advanced Talents of Shenzhen University (Grant no. 000070) and Ningbo Innovation and Entrepreneurship Funding for Study Abroad Personnel (2012B72018).

References

[1] T. Weise, S. Bouaziz, H. Li, and M. Pauly, "Realtime performance-based facial animation," *ACM Transactions on Graphics*, vol.30, no.4, pp. 77, 2011.

[2] I. Kotsia and I. Pitas, "Facial Expression Recognition in Image Sequences Using Geometric Deformation Features and Support Vector Machines," *IEEE Transactions on Image Processing*, vol.16, no.1, pp. 172-187, 2007.

[3] G. Pan, S. Han, Z. Wu, and Y. Zhang, "Removal of 3D facial expressions: A learning-based approach," in *Proc. Computer Vision and Pattern Recognition (CVPR)*, 2010, pp. 2614-2621.

[4] F. Al-Osaimi, M. Bennamoun, and A. Mian, " An expression deformation approach to non-rigid 3D face recognition," *International Journal of Computer Vision*, vol.81, no.3, pp. 302-316, 2009.

[5] Y. Wang, G. Pan, and Z. Wu, "3D face recognition in the presence of expression: A guidance-based constraint deformation approach," in *Proc. Computer Vision and Pattern Recognition, 2007. CVPR '07. IEEE Conference on*, 2007, pp. 1-7.

[6] D. Beymer, A. Shashua, and T. Poggio, 'Example based image analysis and synthesis," Artificial Intelligence Laboratory, Massachusetts Institute of Technology, A.I. Memo No. 1431, 1993.

[7] Q. S. Zhang, Z. C. Liu, B. N. Guo, D. Terzopoulos, and H. Y. Shum, "Geometry-driven photorealistic facial expression synthesis," *IEEE Transactions on Visualization and Computer Graphics*, vol.12, no.1, pp. 48-60, 2006.

[8] D. Huang and F. De la Torre, "Bilinear kernel reduced rank regression for facial expression synthesis," in *Proc. Proceedings of the 11th European conference on Computer vision: Part II*, 2010, pp. 364-377.

[9] A. Raouzaiou, N. Tsapatsoulis, K. Karpouzis, and S. Kollias, "Parameterized facial expression synthesis based on MPEG-4," *EURASIP Journal on Applied Signal Processing*, vol.2002, no.1, pp. 1021-1038, 2002.

[10] Z. Liu, Y. Shan, and Z. Zhang, "Expressive expression mapping with ratio images," in *Proc. Proceedings of the 28th annual conference on Computer graphics and interactive techniques*, 2001, pp. 271-276.

[11] Y. H. Zhang, W. Y. Lin, B. Zhou, Z. Z. Chen, B. Sheng, and J. X. Wu, "Facial expression cloning with elastic and muscle models," *Journal of Visual Communication and Image Representation*, vol.25, no.5, pp. 916-927, 2014.

[12] M. L. Song, Z. Dong, C. Theobalt, H. Q. Wang, Z. C. Liu, and H. P. Seidel, "A generic framework for efficient 2-d and 3-d facial expression analogy," *IEEE Transactions on Multimedia*, vol.9, no.7, pp. 1384-1395, 2007.

[13] K. Li, Q. H. Dai, R. P. Wang, Y. B. Liu, F. Xu, and J. Wang, "A data-driven approach for facial expression retargeting in video," *IEEE Transactions on Multimedia*, vol.16, no.2, pp. 299-310, 2014.

[14] K. Qian, B. Wang, and H. Chen, "Automatic flexible face replacement with no auxiliary data," *Computers & Graphics*, vol.45, no.0, pp. 64-74, 2014.

[15] J. Liao, R. S. Lima, D. Nehab, H. Hoppe, P. V. Sander, and J. H. Yu, "Automating image morphing using structural similarity on a halfway domain," *ACM Transactions on Graphics*, vol.33, no.5, pp. 168, 2014.

[16] S. Ren, X. Cao, Y. Wei, and J. Sun, "Face alignment at 3000 FPS via regressing local binary features," in *Proc. IEEE Conference on Computer Vision and Pattern Recognition*, 2014.

[17] V. Kazemi and S. Josephine, "One millisecond face alignment with an ensemble of regression trees," in *Proc. IEEE Conference on Computer Vision and Pattern Recognition*, 2014.

[18] T. Beier and S. Neely, "Feature-based image metamorphosis," in *Proc. ACM SIGGRAPH Computer Graphics*, 1992, pp. 35-42.

[19] Y. L. Weng, W. W. Xu, Y. Wu, K. Zhou, and B. N. Guo, "2D shape deformation using nonlinear least squares optimization," *The Visual Computer*, vol.22, no.9-11, pp. 653-660, 2006.

[20] C. Larboulette and M. P. Cani, "Real-time dynamic wrinkles," in *Proc. Proceedings of the Computer Graphics International*, 2004, pp. 522-525.

[21] Y. Bando, T. Kuratate, and T. Nishita, "A simple method for modeling wrinkles on human skin," in *Proc. Proceedings of the 10th Pacific Conference on Computer Graphics and Applications*, 2002, pp. 166.

[22] P. Debevec, "Rendering synthetic objects into real scenes: Bridging traditional and image-based graphics with global illumination and high dynamic range photography," in *Proc. ACM SIGGRAPH 2008 classes*, 2008, pp. 32.

[23] T. F. Cootes, C. J. Taylor, D. H. Cooper, and J. Graham, "Active shape models-their training and application," *Computer Vision and Image Understanding*, vol.61, no.1, pp. 38-59, 1995.

[24] A. Asthana, S. Cheng, and M. Pantic, "Robust discriminative response map fitting with constrained local models," in *Proc. IEEE Conference on Computer Vision and Pattern Recognition*, 2013.

[25] P. Lucey, J. F. Cohn, T. Kanade, J. Saragih, Z. Ambadar, and I. Matthews, "The Extended Cohn-Kanade Dataset (CK+): A complete dataset for action unit and emotion-specified expression," in *Proc. Computer Vision and Pattern Recognition Workshops (CVPRW)*, 2010, pp. 94-101.

[26] S. M. Seitz and C. R. Dyer, "View morphing," in *Proc. Proceedings of the 23rd Annual Conference on Computer Graphics and Interactive Techniques*, 1996, pp. 21-30.

[27] V. Blanz, C. Basso, T. Poggio, and T. Vetter, " Reanimating faces in images and video," *Computer Graphics Forum*, vol.22, no.3, pp. 641-650, 2003.